



12th International Conference on Vibration Problems, ICOVP 2015

Gearbox Fault Detection using Synchro-squeezing Transform

Budhaditya Hazra^{a*} and Sriram Narasimhan^{b*}

^aAssistant professor, department of Civil Engineering, IIT-Guwahati, India.

^bAssociate professor, department of Civil and Environmental Engineering, University of Waterloo, Canada.

Abstract

This paper presents a novel fault-detection method for gearbox vibration signatures using synchro-squeezing transform (SST). Premised upon the concept of time-frequency (TF) reassignment, SST provides a sharp representation of signals in TF plane compared to many popular TF methods. Additionally, it can also extract the individual components, called intrinsic mode functions or IMFs, of a non-stationary multi-component signal, akin to empirical mode decomposition. The rich mathematical structure based on continuous wavelet transform makes SST a promising candidate for gearbox diagnosis. This work utilizes the decomposing power of SST to extract the IMFs from gearbox signals. For robust detection of faults in gear-motors, a fault detection technique based on time-varying autoregressive coefficients of IMFs as features is utilized. Sequential Karhunen-Loeve transform is employed on the condition indicators to select the appropriate window sizes on which SST can be applied. Laboratory experimental data obtained from drivetrain diagnostics simulator provides test bed to demonstrate the robustness of the proposed algorithm.

© 2016 The Authors. Published by Elsevier Ltd. This is an open access article under the CC BY-NC-ND license (<http://creativecommons.org/licenses/by-nc-nd/4.0/>).

Peer-review under responsibility of the organizing committee of ICOVP 2015

Keywords: Synchro-squeezing transform (SST); Sequential Karhunen-Loeve transform (SKLT); time-varying auto-regressive model (TVAR)

1. Introduction

Gearboxes are critical components in industrial rotating machinery infrastructure, whose failures can cause severe outages leading to substantial monetary losses and expensive breakdown maintenance. To ensure smooth operation of gearboxes and to reduce their maintenance costs, an efficient fault detection framework is necessary. In this study, a novel fault detection scheme based on the recently developed concepts of SST [1] in conjunction with

* Corresponding author. Tel.: +91-361-258-3334; fax: +91-361- 258 2440.

E-mail address: budhaditya.hazra@iitg.ernet.in

rotating machinery condition indicators and time-varying auto-regressive coefficients is presented to assess the condition of gearboxes. SST is an efficient signal decomposition tool, by the use of which gear meshing frequencies are readily extracted from the raw vibration signal. Current literature on SST in gearbox diagnostics is limited to those utilizing its re-assignment capability [2]. The proposed method [17] can track streaming data in non-stationary environments as opposed to the current practice of the use of subjective windowing. A combination of CI and SKLT in an integrated framework with the application of time varying autoregressive coefficients is to detect faults

2. Literature review

Traditionally gearbox diagnostics involved a direct application of time and frequency domain methods to the gearbox signals, followed by the use of condition indicators [10]. Spectral analysis based on Fourier transform, cepstrum, and envelope spectrum, etc., have been reported extensively [5]. To cater to non-stationarity, short-time Fourier transform (STFT) [5], wavelet transform [9], Cohen's class distributions [4] have also been used. In parametric approaches, auto-regressive modeling has been applied using both time-invariant [5] and time varying approaches using Kalman filtering [12]. Signal decomposition methods such as empirical mode decomposition (EMD) [6] and its refinements has partly allayed the problems associated with the application of traditional techniques. However, EMD based methods suffer from issues such as poor separation of closely spaced modes, mode mixing, poor performance in noisy environments, which degrades its performance in rotating machinery diagnosis [6]. SST [1, 2] is a relatively new and promising signal processing tool capable of decomposing noisy non-stationary signals into its individual components (also called intrinsic mode functions, or IMFs), providing an attractive alternative to the former approach. In the present work, this decomposition facet of SST is exploited to extract key IMFs from gearbox signals and incorporate them within the framework of fault detection. Signal processing generates multiple classes of diagnostic patterns depending on the severity of faults. These patterns need to be interpreted through condition measures using inference tools like pattern recognition [14], classification anomaly detection etc. [15]. The fault detection part comprises of a two-steps: (i) decomposition of vibration signatures into key time-frequency components (IMFs) using SST. (ii) Processing the IMFs through a time-varying auto-regressive modeling to generate features that can detect faults and their severity. The time-varying auto regressive (TVAR) coefficients estimated using the Kalman filter [13]. The statistical variations of the AR coefficients reflect the non-stationary characteristics that arise due to the occurrence of defect or deterioration.

The overall approach (shown in Figure 1) in this study consists of two stages: the pre-processing stage where condition indicators are used to select the appropriate window sizes, followed by the signal-processing stage where SST and TVAR modeling operates on the selected windows. Recursive condition indicators and SKLT are used for window selection and the complete execution of this step is online. Following this two-stage approach allows us to limit the computationally intensive SST to the interesting portions of the data, and can be performed offline. TVAR scheme using Kalman estimation is applied for anomaly detection. In the proposed method, streaming data can be tracked in non-stationary environments as opposed to the current practice of subjective windowing. The use of CI's and SKLT in an integrated framework is one of the key contributions of this work.

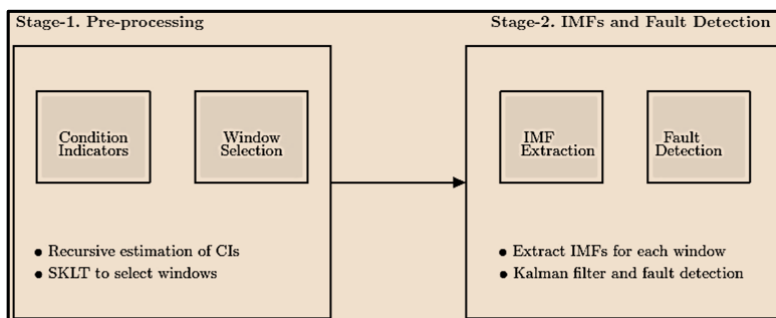


Figure 1. Overall approach

3. Background

3.1. Synchro-squeezing transform

Introduced in the context of speech signals [1], synchro-squeezing has emerged as an EMD-like tool capable of extracting AM-FM components resembling intrinsic mode functions (IMFs). It works by reallocating the CWT coefficients based on the frequency information, to obtain a sharper or ‘squeezed’ picture in the time-frequency plane much like time-frequency reassignment, from which the instantaneous frequencies can be extracted. Since synchro-squeezing is primarily based on continuous wavelet transform (CWT), it is worthwhile to define the CWT of a signal $s(t)$ first expressed as follows:

$$W_s = \frac{1}{a} \int_{\mathbb{R}} s(t) \overline{\psi\left(\frac{t-b}{a}\right)} dt. \quad (1)$$

where, $\psi(t)$ is the mother wavelet, a and b are scale and shift parameters, respectively. In the context of synchrosqueezing, it is necessary for the mother wavelet to have a unique peak frequency [14]. The basic idea of synchrosqueezing is best understood by considering a purely harmonic sinusoidal signal [1]. The wavelet transform of such a signal should be theoretically concentrated around the frequency of the signal as a line of constant magnitude. However, in practice, it is observed that the wavelet transform is always smudged around the horizontal line corresponding to the sinusoid frequency in the T-F plane. Daubechies *et. al* [1] suggested a way around this problem by proposing the estimation of instantaneous frequency $\omega(a,b)$ for all values of (a, b) , which is given by the following formula:

$$\omega(a,b) = \frac{-i}{W_s(a,b)} \frac{\partial}{\partial b} W_s(a,b) \quad (2)$$

where $W_s(a,b)$ is the CWT of the signal. Implementation-wise the wavelet coefficients in $W_s(a,b)$ are computed only at discrete scales a_k and its synchrosqueezed counterpart $T_s(\omega,b)$ is determined at the centers ω_c of the successive bins $[\omega_c - \frac{1}{2}\Delta\omega, \omega_c + \frac{1}{2}\Delta\omega]$, by the following formula [1]:

$$T_s(\omega_c,b) = \frac{1}{\Delta\omega} \sum_{a_k: |\omega(a_k,b) - \omega_c| \leq \frac{\Delta\omega}{2}} W_s(a_k,b) a_k^{-3/2} \Delta a_k. \quad (3)$$

The next step in the synchrosqueezing transform is extraction of the IMFs. This involves extraction of one ‘‘ridge’’ from T_s by finding the curve $c(t)$ with the largest energy subject to some optimization criterion [8]. Once the curve $c(t)$ is known, the associated mode h can be estimated by summing the synchrosqueezed transform near that curve: at time t , according to the following equation:

$$h(t) = \int_{\omega \approx c(t)} T_s(\omega,t) d\omega \quad (4)$$

In the present work, the authors follow the approach proposed by [8]. The details of implementation of the procedure are beyond the scope of this work and the readers are referred elsewhere for details [8].

3.2. Online window selection

Condition indicators are statistical indicators of signal quality, which are traditionally used in gearbox diagnosis. For online monitoring applications, a direct application of SST on raw vibration data is computationally intensive. Hence, in the present study a two-stage process is adopted, where the first stage is a preliminary pre-processing step wherein the windows of SST operation are selected using a variety of condition indicators. This approach is motivated for the situations where there are frequent changes in the operating conditions that do not necessarily correspond to damage. To detect the condition of the gears and bearings, 6 condition indicators [10] which have

been widely used in the literature, are chosen, namely: variance, kurtosis, crest factor and the energy operator. Only a brief description of the performance indicators is provided in Table. 1.

Table 1. Condition Indicators

Condition indicator	Formula
Variance	$\sigma^2(s) = \frac{1}{N} \sum_{i=1}^N (s(t_i) - \mu)^2$
Kurtosis	$\kappa(s) = \frac{1}{N} \sum_{i=1}^N \frac{(s(t_i) - \mu)^4}{\sigma^4}$
Normalized sixth moment	$SM(s) = \frac{1}{N} \sum_{i=1}^N \frac{(s(t_i) - \mu)^6}{\sigma^6}$
Energy operator	$EOP = s(i)^2 - s(i + 1)s(i - 1)$
Crest factor	$CF = \frac{\max(x(i)) - \min(x(i))}{\sigma}$

For online window selection it is important that the condition indicators are estimated recursively [17]. The next step in window selection is the application sequential Karhunen-Loeve transform (SKLT) [16] to the estimated recursive condition indicators.

The main idea here is that changes in the characteristics of data due to a change in the gearbox health states are captured through recursive singular value decomposition (SVD). SKLT is applicable to low dimensional approximation of principal component analysis, i.e., where one or at most 2 principal components are expected. The main objective is that given a set of vectors, one seeks to estimate a set of orthogonal unit vectors such that the projections of data on the subspace spanned by the vectors approximate the input vectors best in a mean square error sense. Consider a $p \times q$ data matrix α for which singular value decomposition $\alpha = \mathbf{U}\mathbf{\Lambda}\mathbf{V}^T$ has been already computed. When a new $p \times (q + r)$ matrix β of r new observations becomes available, the goal is to compute the SVD of $[\alpha \ \beta] = \mathbf{U}^*\mathbf{\Lambda}^* \mathbf{V}^{*T}$. Since SKLT is based on the computation of \mathbf{U}^* and $\mathbf{\Lambda}^*$ only \mathbf{V}^* is not estimated. For the details of the exposition of the algorithm, the readers are referred elsewhere [16, 17].

3.3 Fault detection using TVAR modeling

Fault detection involves detecting deviations from a baseline health condition. In most cases, it adequately serves the need for a trigger to perform inspection or a maintenance action. In the present context time varying autoregressive (TVAR) coefficients of the IMFs extracted using SST are employed to detect fault in the gearmotors to facilitate the use of low-order model. Such a model tracks the real-time changes of the model coefficients which reveal the mechanical faults in the system. Let $y(n)$ represent the estimated IMF, $v(n)$ denotes the zero-mean Gaussian measurement noise with variance σ_v^2 . Then the AR model of order p can be represented as:

$$y(n) = \sum_{k=1}^p a_k y(n - k) + v(n) \tag{5}$$

However, since the IMFs are expected to be non-stationary in nature, their modeling requires a time-varying approach for which the Kalman filter (KF) is employed as a sequential estimator that estimates the hidden states (AR model coefficients). Assuming that the AR coefficients are the hidden states of the system, the TVAR model can be written in following discrete form:

$$x(n) = \Gamma(n - 1) x(n - 1) + w(n) \tag{6.1}$$

$$y(n) = C(n) x(n) + v(n) \tag{6.2}$$

where $\mathbf{x}(n) = [a_1(n), a_2(n), \dots, a_p(n)]^T$ is the unknown state vector, which corresponds to the AR coefficients at the discrete-step n . The matrix Γ is assumed to be an identity matrix. $\mathbf{C}(n) = [y(n), y(n), \dots, y(n-p)]^T$ is the observation vector, $\mathbf{w}(n)$ represents the process noise with the covariance $\mathbf{P}_w = I\sigma_w^2$ that is uncorrelated with $\mathbf{v}(n)$. The estimated states (i.e., AR coefficients) and their covariance from the individual IMFs are utilized as features, which are then monitored under different condition states of the gearbox. In addition to the AR coefficient, the trace of state covariance matrix \mathbf{P}_x is also used as an indicator to the extent of sidebands appearing in the gearbox meshing frequencies [17].

4. Case study with laboratory experimental data

The primary test-bed to demonstrate the methodology is a system called drivetrain dynamic simulator (DDS). The DDS is designed by SpectraQuest Inc to simulate industrial drivetrains for experimental research. Figure. 2 shows a drivetrain simulator that is designed for studying common gearing faults. The gearbox is driven by a variable frequency drive (VFD) induction motor which is controlled by a programmable controller with a display panel showing input speeds and a tachometer showing the rpm of the input shaft. The elements of the DDS are designed such that a variety of configurations can be tested.

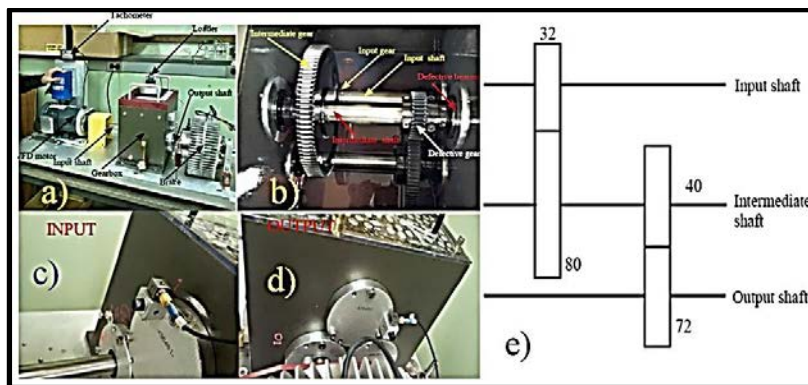


Figure 2. a) DDS; b) Location of faulty gear; c) & d) sensor locations; e) gear-meshing diagram

The line diagram of the gear meshing is shown in figure. 2e. On the output section the 40 teeth gear on the intermediate shaft meshes with the 72 teeth gear on the output shaft. For the present study a variety of fault conditions were simulated by suitable replacement of 40 teeth gear with its chipped tooth replica. Tests were run for various steady input speeds starting from 10 Hz, 20 Hz and 40 Hz. The brake used in DDS is of particle magnetic type and has a torque range of 1-30 lb-ft. For the present study, a braking torque equivalent to 3 Volts (approximately 4 lb-ft) is applied and the data is collected for a combination of 6 conditions of change in rpm, presence/absence of brakes, and the presence/absence of a chipped tooth (50%) fault in the 40 tooth gear. The details of states of data are explained in table. 2. A key point to note here is that the different states of data are concatenated end to end to represent close to a real industrial drive-train that goes through changes in operating and health conditions.

Two Dytran 3263A2 triaxial accelerometers mounted on the input side and output side of the intermediate shaft are used. The position of the accelerometers, their axes and orientation is shown in figure 1. The accelerometer channels are labelled as follows: the X, Y and Z channels on the input side are labelled as 1, 2 and 3 and the corresponding counterparts on the output side as 4, 5 and 6. The sampling frequency is set to 10 KHz. Providing an input signal of 20 Hz at the VFD controller does not translate into an exact 20 Hz input RPM, in fact it is 19.43 Hz for the present case.

Table 2. States of data for the experimental set-up

STATE	Data range(in 1000's)	Fault state	Braking state	RPM
1	1-50	NO	3V	10
2	50-100	NO	NO	20
3	100-150	NO	3V	20
4	150-200	Chipped	NO	20
5	200-250	Chipped	3V	20
6	250-300	Chipped	3V	40

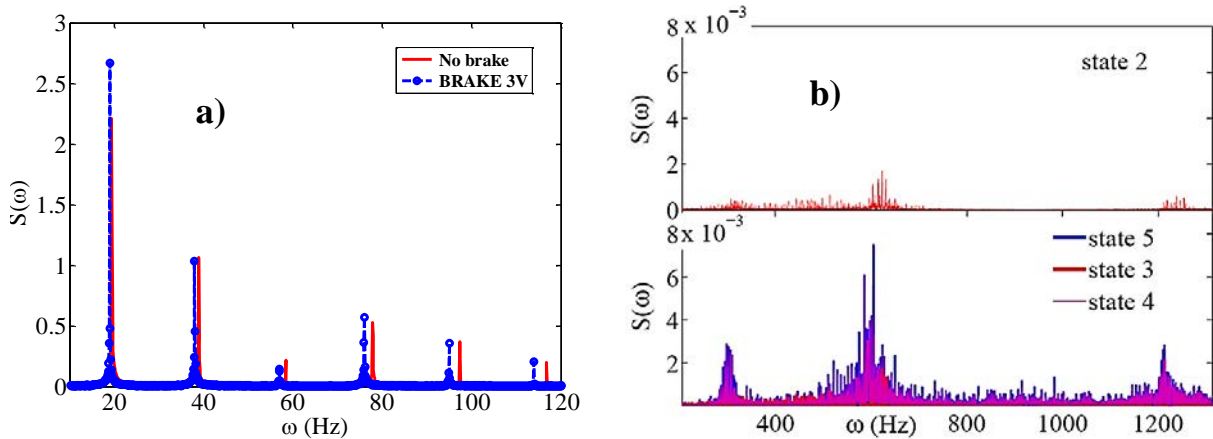


Figure 3. Fourier spectrum of the a) tachometer signal and b) DDS signal

Application of brakes further reduces the speed to 18.98 Hz. Fourier spectra of the tachometer data in figure. 3 clearly show peaks at 19.43Hz, 18.98 Hz and their multiples. The Fourier spectrum of the channel-3 is shown in figure. 3 for an input speed of 20Hz. Harmonics can be clearly observed at the multiples of 310 and 621Hz. Between the spectra of the chipped tooth and the no fault cases, it is easy to observe the relative differences in the energy content in the frequency domain, which can be attributed to the presence of relatively large sidebands for the chipped tooth case. SST applied to channel-3 data (Figure. 4a) yields 6 IMFs for the new and old states. Of these, two key ones that have significant energy and common occurrence between the chipped and the good gears are shown. It can be clearly observed that IMFs corresponding to the chipped gear have significantly more energy and width corresponding to the sidebands. Moreover, it can be observed that there is a frequency shift between the no brake and 3V brake states owing to the decrease in rpm resulting from braking.

Condition indicators plotted for the channels 3, 4 and 5 is shown in figure. 4b. It can be observed that there is a considerable jump in the CI values after approximately the first 50000 samples of data. These samples represent the data obtained from the gearbox in state-1. The remaining portion of CIs represents data between states 2 to 6. Although the change of states in the data from state-1 to the others is quite obvious, the trend in the values of the condition indicators is ambiguous especially towards the later portions of the data. However, the trend of the values of kurtosis, sixth order moment (SM), CF and EOP-variance is less obvious, which makes it difficult to assess the state of the data through visual inspection. Figure. 5 shows the windows generated by application of SKLT on CI's. It shows 6 partitions some of which are not so obvious just by looking at the data. The key observation from Figures. 4b and 5 is that, it is not possible to discern all of the 6 states from condition indicators alone or for that matter any one particular channel. All the states are hidden in this (6 x 3) multichannel condition indicator space. To

obtain more definitive conclusions it is important to present a complete picture, TVAR modelling and PCA based clustering is used as explained next.

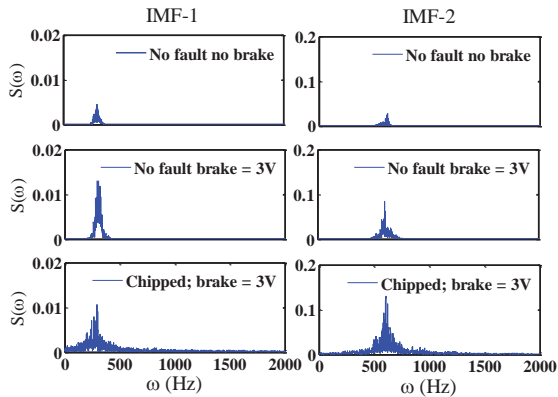


Figure 4a. Fourier spectra of the IMFs

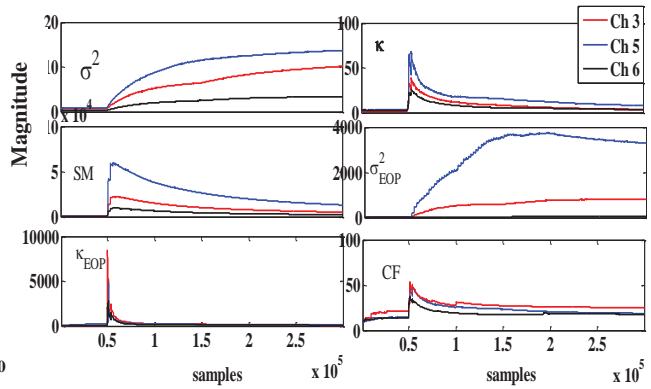


Figure 4b. Recursive condition indicators for the DDS data

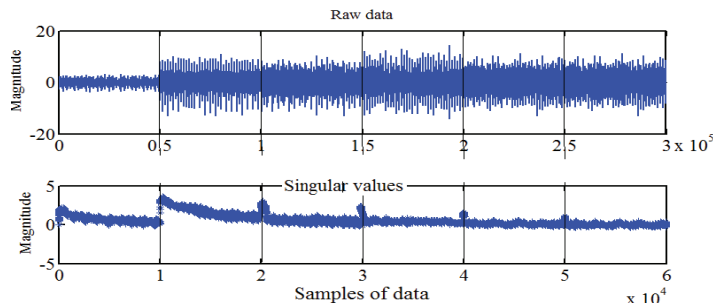


Figure 5. Online window selection for the DDS data

Fault detection is performed by fitting TVAR-2 (Eq. 6) models to the three key IMFs (from each of the channels 3, 4 and 6) for each of the partitioned windows. For each window the 9 column vectors corresponding to the variances of and the trace vectors of covariance matrices are utilized to perform principal component analysis. The cluster plot between the first 2 major principal components is plotted in **Figure. 6**. It can be observed that the spread of the scatter varies very slightly for the first 3 windows indicating thereby that the gear has not chipped in the selected windows. From the window-4 onwards, there is a significant change in the spread of the clusters compared to the first 3 windows which indicates that some alteration in gear health state has occurred in the regime starting from window 4, which corroborates with the physical condition that the gear is chipped starting from the 4th state. Between windows 4 to 6, the spread increases marginally indicating that the last 3 partitions in figure. 5 do not correspond to different health states. They are indicative of changes in operating conditions (changes in braking state and RPM) not associated with damage. Hence, it can be easily inferred that there are two distinct health states that are identified by the cluster diagram of resulting from the TVAR modelling. Thus, it is safe to conclude that the proposed method successfully demonstrates the fault detection in a damaged gearbox.

4. Conclusions

A new fault detection algorithm towards condition monitoring of gearmotors using a combination of synchro-squeezing transform, rotating machine condition features, sequential Karhunen Loeve transform and TVAR modeling is presented. The reassignment property of synchro-squeezing transform allows for a better resolution of

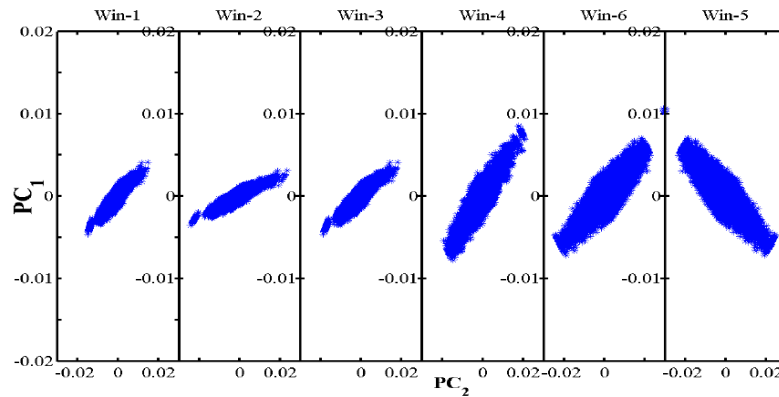


Figure 6. Cluster diagram for the DDS data

the signal features in the presence of noise. Subsequent application of curve extraction techniques along the ridges allowed EMD like decomposition of the signal into IMFs. Application of recursive condition indicators on the raw data in conjunction with the use sequential Karhunen-Loeve transform facilitated an automated framework for the selection of optimal window size for fault detection, more effective than subjective windowing. Application of Kalman filter based TVAR modelling of the IMFs for each of the selected windows, delineated the normal and chipped gear states in drivetrain diagnostic simulator in varied operating conditions. Results prove that the proposed approach results in successful fault diagnosis and works well when used with experimentally acquired data.

References

1. Daubechies, I., Lu, J., and Wu, H. (2011). Synchrosqueezed wavelet transforms: An empirical mode decomposition-like tool. *Applied and Computational Harmonic Analysis*, 30(2), pp. 243–261.
2. Liang, M., and Li, C. (2012). A generalized synchro-squeezing transform for enhancing signal time–frequency representation. *Signal Processing*, 92(9), pp. 2264–2274.
3. Antoni, J. and Randall, R. B. (2011). Rolling element bearing diagnostics—A tutorial. *Mechanical Systems and Signal Processing*, 25(2), pp. 485–520.
4. Cohen, L. (1995). *Time-Frequency Analysis*. Prentice-Hall, Englewood Cliffs, NJ, USA.
5. Jardine, A. K. S., Lin, D., and Banjevic, D. (2006). A review on machinery diagnostics and prognostics implementing condition based maintenance. *Mechanical Systems and Signal Processing*, 20(7), pp. 1483–1510.
6. Lei, Y., Lin, J., He, Z., and Zuo, M. J., (2013). A review on empirical mode decomposition in fault diagnosis of rotating machinery. *Mechanical Systems and Signal Processing*, 35(1-2), pp. 108–126.
7. Liang, M., and Li, C. (2012). A generalized synchro-squeezing transform for enhancing signal time–frequency representation. *Signal Processing*, 92(9), pp. 2264–2274.
8. Oberlin, T., Meignen, S., and Perrier, V. (2012), On the Mode Synthesis in the Synchrosqueezing method. Proceedings of EUSIPCO, Bucharest, Aug. 27–31.
9. Staszewski, W., Worden, K., and Tomlinson, G. (1997). Time frequency analysis in gearbox fault detection using the Wigner-Ville distribution and pattern recognition. *Mechanical Systems and Signal Processing*, 11(5), pp. 673–692.
10. Vecer, P., kreidl, M., and Smid, R. (2005). Condition indicators for gearbox condition monitoring systems. *Acta Polytechnica*, 45(6), pp. 35–43.
11. Wang, W. and McFadden, P. (1995). Application of orthogonal wavelets to early gear damage detection. *Mechanical Systems and Signal Processing*, 9(5), 497–507.
12. Zhan, Y. and Jardine, A. (2005). Adaptive autoregressive modeling of non-stationary vibration signals under distinct gear states Part 1: modeling. *Journal of Sound and Vibration*, 286(6), 429–450.
13. Nguyen, D. P., Wilson, M. A., Brown, E. N., and Barbieri, R. (2009). “Measuring instantaneous frequency of local field potential oscillations using the kalman smoother.” *Journal of Neuroscience Methods*, 184(2), 365 – 374.
14. Vachtsevanos, G., Lewis, F., Roemer, M., Hess, A., and Wu, B. (2006). *Intelligent fault diagnosis and prognosis for engineering systems*. John Wiley and Sons, NJ, USA.
15. Timusk, M., Lipssett, M., and Mechefske, C. K. (2008). “Fault detection using transient machine signals.” *Mechanical Systems and Signal Processing*, Elsevier, 22(7), 1724–1749.
16. Ross, A. D., Lim, J., Lin, R., and Yang, M. T. (2008). “Incremental learning for robust visual tracking.” *International Journal of Computer Vision*, Springer, 77(1-3), 125–141.
17. Hazra B, Narasimhan S, Sadhu A (2015), Fault detection of gearboxes using synchro-squeezing transform. *Journal of Vibration and Control*, accepted for publication.